PHYSICAL REVIEW D **86,** 122004 (2012)

Creep events and creep noise in gravitational-wave interferometers: Basic formalism and stationary limit

Yuri Levin[1,2,*]

[1]*Monash Center for Astrophysics, Monash University, Clayton, VIC 3800, Australia*
[2]*Leiden Observatory, Leiden University, Niels Bohrweg 2, 2300 RA Leiden, The Netherlands*
(Received 27 October 2012; published 19 December 2012)

In gravitational-wave interferometers, test masses are suspended on thin fibers which experience considerable tension stress. Sudden microscopic stress release in a suspension fiber, which I call a ''creep event,'' would excite motion of the test mass that would be coupled to the interferometer's readout. The random test-mass motion due to a time sequence of creep events is referred to as ''creep noise.'' In this paper I present an elastodynamic calculation for the test-mass motion due to a creep event. I show that within a simple suspension model, the main coupling to the optical readout occurs via a combination of a ''dc'' horizontal displacement of the test mass and excitation of the violin and pendulum modes, and not, as was thought previously, via lengthening of the fiber. When the creep events occur sufficiently frequently and their statistics is time independent, the creep noise can be well approximated by a stationary Gaussian random process. I derive the functional form of the creep noise spectral density in this limit, with the restrictive assumption that the creep events are statistically independent from each other.

DOI: 10.1103/PhysRevD.86.122004 PACS numbers: 04.80.Cc

I. INTRODUCTION

Gravitational-wave interferometers like the Laser Interferometric Gravitational-wave Observatory (LIGO) in the United States of America [1], VIRGO [2] in Europe, and their smaller counterparts GEO600 in Germany [3] and TAMA in Japan [4], are using superprecise optomechanical measurements to search for astrophysical gravitational waves. After several years of taking scientific data, LIGO and VIRGO are currently being upgraded with improved instrumentation and should again become operational in 2015 [5,6]. LIGO Science Collaboration (LSC) and the VIRGO community are projecting [7] that with the upgraded technology, both interferometers will soon be measuring multiple coalescences of relativistic compact objects (neutron stars and black holes). These projections are based in part on the theoretical predictions for spectral density of the interferometers' noise. It is thought that the random processes that contribute most of the noise, i.e., the seismic shaking of the suspensions [8], the thermomechanical and thermorefractive fluctuations of the mirror surface [9], and the quantum-mechanical fluctuations of the light field coupled to the test-mass motion [10,11] are well understood [12].

One of the dangerous unknowns for the advanced gravitational-wave interferometers is a non-Gaussian noise from a superposition of transient events in the instrument. In this paper I concentrate on the creep noise, which is caused by a superposition of the sudden localized tension stress releases (creep events) in suspension fibers and their end attachments. It has been thought that a creep event would couple to the interferometer's readout via lengthening of the fiber [16]. Specifically, it was argued that because of Earth's curvature, the laser beam was not strictly perpendicular to the suspension fiber, and thus the fiber's lengthening would result in some test-mass displacement along the beam. In this paper I show that this coupling, while present, is not dominant, at least for a simple model where the fiber is represented by a cylinder with constant radius. Instead, a creep event couples to the interferometer's output predominantly through excitation of the pendulum and violin modes of the suspension; this coupling is explicitly calculated in this work.

The fact that creep events couple to the transverse vibrational modes of the system is in agreement with the experiment of Ageev *et al.* [17] who find a substantial excess noise in the transverse motion of a tungsten wire stretched to 20% of the breakup stress. Similar excess noise in steel wires was observed in Ref. [18]. However, the results in Ref. [17] were not confirmed by Gretarsson and Saulson [19] who did not observe any excess noise in the motion of the stressed tungsten wire. Moreover, it is far from obvious that the processes responsible for the creep events in metallic fibers [20] will be operating in the fused silica suspension fibers such as the ones that are currently used in GEO600 and that will be used in the advanced LIGO, VIRGO, and KAGRA suspensions [21]. Two experiments with fused silica fibers have been performed in Refs. [19,22]; in both experiments no excess noise was discovered near the violin resonant frequency of the fiber. In a more recent work [23], the motion of a test mass was monitored in GEO600, where the fused silica suspension fibers were used. The motion near the violin-mode frequency was entirely consistent with that of the thermally excited violin mode. Therefore, currently there is no experimental evidence that the creep excess noise in the

*yuri.levin@monash.edu.au

future advanced gravitational-wave interferometers will pose a serious problem. However, there are at least two reasons to keep investigating the creep noise: (1) the measurements in Refs. [19,22,23] have all been performed at frequencies from several hundreds to thousands of hertz, where the noise of ground-based interferometers is strongly dominated by the quantum shot noise, while the danger from creep noise exists at much lower frequencies, in the same region of tens of hertz where the shot noise is unimportant; and (2) the main source of creep noise may well not be inside the fused silica suspension fibers, but inside other carrying parts of the system like the bond between the test masses and the "ears" that are supporting them [24,25]. It is thus important to understand how a creep event inside the suspension couples to the horizontal motion of the test-mass, as well as the frequency dependence of the noise generated by a multitude of the creep events. This paper lays a theoretical foundation for addressing these issues.

The plan of the paper is as follows. In Sec. II, I present a convenient reciprocity relationship for linear elastodynamic systems. In Sec. III, I use this relationship to derive the interferometer's response to a creep event, as a function of the location of the stress release in the fiber. In Sec. IV, I derive the functional form of the creep noise spectral density, in the limit where the creep noise can be treated as a stationary Gaussian random process. A brief discussion of the future work is presented in Sec. V.

II. ELASTODYNAMICS AND RECIPROCITY THEOREM

During the creep event, the stress changes suddenly in some small volume of the fiber. But how does this affect the motion of the test mass? At first glance, this seems like a formidable problem in elastodynamics. However, it turns out that solving the reciprocal problem is sufficient. Namely, one should in a mental experiment apply a sudden force to the test mass and compute the motion of the fiber at the location where the creep event originated. The solution of the reciprocal problem leads directly to the solution of the original problem. Reciprocity relations have been thoroughly studied in elastodynamics; see e.g., Ref. [26] for a comprehensive review. Here I will use the following formulation of the reciprocity theorem.

Consider an elastodynamic system initially at rest, that is being driven by a distributed force, with the force per volume given by

$$\vec{F}(\vec{r}, t) = \vec{f}(\vec{r})\chi(t), \tag{1}$$

where $\chi(t)$ is some function that is nonzero only for $t > 0$. Consider also a readout variable

$$X(t) = \int d^3 r \vec{g}(\vec{r}) \cdot \vec{\xi}(\vec{r}, t), \tag{2}$$

where $\vec{\xi}(\vec{r}, t)$ is the displacement from rest at location $\vec{r}$ and time t. Both the applied forces and displacement are assumed to be small, so that a linear approximation of elastodynamics holds. The reciprocity theorem states that if in the pair of Eqs. (1) and (2) the form factors $\vec{f}(\vec{r})$ and $\vec{g}(\vec{r})$ are interchanged then the readout variable $X(t)$ remains the same. In other words, the input-output dynamical system is invariant with respect to $\vec{f}$ and $\vec{g}$ interchange, with $\chi(t)$ being the input and $X(t)$ being the output.

The proof of the theorem is as follows. Let $\vec{\xi}_n(\vec{r})$ be the normal modes of the system, with proper angular frequencies ω_n. A displacement field $\vec{\xi}$ can then be decomposed into a series

$$\vec{\xi}(\vec{r}, t) = \Sigma_n a_n(t)\vec{\xi}_n(\vec{r}). \tag{3}$$

The mode amplitudes $a_n(t)$ are the new dynamical coordinates. The Lagrangian of the unforced system is given by

$$L_0 = \frac{1}{2}\Sigma_n m_n[\dot{a}_n^2 - \omega_n^2 a_n^2], \tag{4}$$

where m_n is the effective mass of the nth mode. External forcing of Eq. (1) is introduced via an additional interaction Langangian term

$$L_{\text{int}} = \int d^3 r \vec{F}(\vec{r}, t) \cdot \vec{\xi}(\vec{r}, t), \tag{5}$$

which, in terms of the coordinates a_n, can be rewritten as

$$L_{\text{int}} = \Sigma_n a_n f_n \chi(t). \tag{6}$$

Here f_n are constants given by

$$f_n = \int d^3 r \vec{\xi}_n(\vec{r}) \cdot \vec{f}(\vec{r}). \tag{7}$$

The full Langrangian allows us to immediately obtain the equations of motion:

$$\frac{d^2 a_n}{dt^2} + \omega_n^2 a_n = \chi(t)\frac{f_n}{m_n}. \tag{8}$$

Therefore,

$$a_n(t) = \frac{f_n}{m_n}\chi_n(t), \tag{9}$$

where $\chi_n(t)$ is the solution to the forced harmonic oscillator problem

$$\frac{d^2 \chi_n}{dt^2} + \omega_n^2 \chi_n = \chi(t) \tag{10}$$

with the initial condition $\chi_n(0) = \dot{\chi}_n(0) = 0$. The readout variable in Eq. (2) can then be written as

$$X(t) = \Sigma_n \frac{g_n f_n}{m_n}\chi_n(t), \tag{11}$$

where g_n is defined similarly to f_n:

$$g_n = \int d^3 r \vec{\xi}_n(\vec{r}) \cdot \vec{g}(\vec{r}). \tag{12}$$

The readout variable $X(t)$ is invariant with respect to the interchange of $\vec{f}$ and $\vec{g}$, Q.E.D.

III. TEST-MASS RESPONSE TO A SINGLE CREEP EVENT

A. General considerations

A creep event happens when a minute section of the suspension fiber refuses to support its full share of the tension stress. What exactly happens microscopically is poorly known, but a simple model will suffice for modeling the elastodynamical behavior. Let us assume that a small fiber element of volume V suddenly does not support any elastic stress T_{ij}. I now consider a slightly reduced elastic system, namely the original one with the small volume element V taken out. This slightly reduced system experiences a sudden force applied to the boundary of the volume element V, so that the boundary surface element $\vec{dS}$, assumed to be directed outside of the volume, experiences the force

$$\vec{dF} = -T_{ij}(\vec{dS} \cdot \vec{e}_j)\vec{e}_i, \tag{13}$$

where $\vec{e}_i$ are the unit vectors along the coordinate axes, and the summation over the dummy indices is assumed.

I would like to evaluate the test-mass displacement $X(t)$ under the action of the force in Eq. (13) that is switched on at $t = 0$ (this situation is somewhat similar physically to the excitation of magnetar motion as a result of sudden reconfiguration of the magnetosphere during a giant magnetar flare; see Ref. [27]). By the reciprocity theorem from the previous section, this is equivalent to acting with the suddenly switched-on force on the test mass, directed along the laser beam:

$$F_{\text{testmass}}(t) = \Theta(t), \tag{14}$$

where $\Theta(t)$ is the Heavyside function [28]. One then has to find the response of the slightly reduced elastic subsystem to this force, and in particular that of the reciprocal readout variable $X_{\text{readout}}(t)$ that is dictated by the functional form of the force in Eq. (13)

$$X_{\text{readout}}(t) = -\int T_{ij}\xi_i \vec{dS} \cdot \vec{e}_j, \tag{15}$$

where the integration domain is the boundary of the volume V. It is obvious that for sufficiently small [29] volume V the response of the slightly reduced system is the same as that of the full system, and from here on I shall make no distinction between the two.

By Gauss's theorem, for small V the above equation can be written as

$$X_{\text{readout}}(t) = -VT_{ij}\frac{\partial \xi_i}{\partial x_j}, \tag{16}$$

where the strain $\partial \xi_i / \partial x_j$ is evaluated at the location of the creep event. To sum up, by finding the response of X_{readout} from Eq. (16) to the force $F_{\text{testmass}} = \Theta(t)$ applied at the test mass along the direction of the laser beam, one finds the test-mass displacement in response to the creep event.

It is convenient and instructive to work in the Fourier domain

$$F_{\text{testmass}}(t) = \int_{-\infty}^{\infty} d\omega F_{\text{testmass}}(\omega) e^{i\omega t}. \tag{17}$$

For the force given by Eq. (14), the force Fourier component is given by

$$F_{\text{testmass}}(\omega) = \lim_{\epsilon \to 0+} \left\{ \frac{1}{2i\pi(\omega - i\epsilon)} \right\}, \tag{18}$$

where positive ϵ serves to avoid the singularity in Eq. (17); the limit $\epsilon \to 0$- would give $F_{\text{testmass}}(t) = \Theta(-t)$.

The test-mass horizontal displacement X_{testmass} under the action of the applied force is given by

$$X_{\text{testmass}}(\omega) = \frac{F_{\text{testmass}}(\omega)}{M} Z[(\omega - i\gamma(\omega)], \tag{19}$$

where the mechanical impedance $Z(\omega)$, as derived in the Appendix, is given by [30]

$$Z[\omega] = \frac{1}{\pi \frac{\omega}{\omega_s} \cot[\pi \frac{\omega}{\omega_s}] \omega_p^2 - \omega^2}. \tag{20}$$

Here, M is the mass of the test mass; $\omega_p = \sqrt{g/l}$ is the pendulum angular frequency of the test mass; $\omega_s = \pi\sqrt{M/(Nm)}\omega_p$ is the fundamental violin-mode angular frequency measured when the test mass is fixed in space; and l, m, and N are the length, the mass, and the number of the strings on which the test mass is suspended, respectively. The small positive $\gamma(\omega) \ll \omega$ inserted into Eq. (19) represent damping. Mathematically, this displaces the poles of $Z(\omega)$ into the upper half of the complex ω plane [31]. These poles represent the frequencies of normal modes of the suspension; their imaginary parts equal the rate of exponential decay of their amplitudes. The actual values of $\gamma(\omega)$ are only important near the normal-mode frequencies and can be measured experimentally.

If no damping is present, the poles of $Z[\omega]$, i.e., the normal-mode frequencies, are given approximately by

$$\omega_0 \simeq \pm\omega_p = \pm\sqrt{g/l} \tag{21}$$

for the pendulum mode, and

$$\omega_{vj} \simeq \pm\left[j\omega_s + (-1)^j \frac{\omega_p^2}{j\omega_s} \right] \tag{22}$$

for the $j = 1, 2, \ldots$ violin modes. Let us introduce nonzero γ_p and γ_{vj} which are the damping rates of the pendulum and violin modes, respectively. The impedance can be expanded as follows:

$$Z(\omega - i\gamma) \simeq \frac{1}{\omega_p^2 - (\omega - i\gamma_p)^2} + \Sigma_{j=1}^{\infty} \frac{2\omega_p^2}{\omega_{vj}^2} \frac{1}{\omega_{vj}^2 - (\omega - i\gamma_{vj})^2}. \quad (23)$$

Substituting Eqs. (20) and (18) into Eq. (19), and evaluating the inverse Fourier transform, I get

$$X_{\text{testmass}}(t) = \frac{1}{M\omega_p^2}[1 - \cos(\omega_p t)e^{-\gamma_p t}] + \Sigma_{j=1}^{\infty} \frac{2\omega_p^2}{M\omega_{vj}^4}[1 - \cos(\omega_{vj} t)e^{-\gamma_{vj} t}]. \quad (24)$$

As expected, the system's response to a sudden force is a constant displacement added to damped oscillations due to excited pendulum and violin modes.

Let us take stock, and sum up what has been done so far. In a reciprocal problem, one has to find out the induced shear at the location of the creep-event source when a sudden force $F(t) = \Theta(t)$ is applied to the test mass. In this subsection I have done part of the problem, i.e., I found the test-mass displacement under the action of the said force. To make further progress, I need to choose a particular model for the suspension fiber itself. In the next subsection I consider one of the particular cases that can be dealt with analytically. The treatment of complicated geometries is left for future work.

B. Example: Creep event in a cylindrical fiber with a constant cross section

Let us consider in detail the case where the creep events occur inside a cylindrical fiber of constant cross section that is rigidly attached at the top to a suspension isolation plate and at the bottom to the test mass. It is assumed here that the allowed test-mass motion is a parallel translation but not rotation, as is the case when four suspension fibers are used. The dominant part of the stress in the fiber is

$$T_{zz} = -\frac{Mg}{N\pi r^2}, \quad (25)$$

where N is the number of suspension fibers and r is the radius of the fibers' horizontal cross section. The readout variable in Eq. (16) is given by

$$X_{\text{readout}} = \frac{MgV}{N\pi r^2} \frac{\partial \xi_z}{\partial z}, \quad (26)$$

where z is the vertical coordinate along the fiber. I choose $z = 0$ at the fiber's top and $z = l$ at the fiber's bottom.

Let x_c, y_c, z be the spatial coordinates of the source of a creep event, where x_c, $y_c = 0$ corresponds to the location of fiber's axis at z, and x_c is measured along the laser beam direction. The vertical strain induced by the fiber's motion is given by (see, e.g., Chapter 11 of Ref. [32])

$$\frac{\partial \xi_z}{\partial z} = -x_c \frac{\partial^2 \eta}{\partial z^2}, \quad (27)$$

where $\eta(z)$ is the horizontal displacement of the fiber. Therefore, the readout variable is

$$X_{\text{readout}} = -\frac{MgVx_c}{N\pi r^2} \frac{\partial^2 \eta}{\partial z^2}. \quad (28)$$

Let us now find the fiber motion $\eta(z, t)$. Its dynamical equation of motion is given by (see, e.g., Chapter 12 of Ref. [32] or Ref. [33])

$$\frac{\partial^2 \eta}{\partial t^2} = c_s^2 \left[\frac{\partial^2 \eta}{\partial z^2} - \lambda^2 \frac{\partial^4 \eta}{\partial z^4}\right]. \quad (29)$$

Here $c_s = \sqrt{Mgl/(Nm)}$ is the velocity of the tension wave in a fiber, and λ is the characteristic bending length given by

$$\lambda = \frac{1}{2}\sqrt{\frac{\pi EN}{Mg}} r^2 = \frac{1}{2}(\xi_{0z,z})^{-1/2} r. \quad (30)$$

Here r is the radius of the fiber, E is the Young modulus, and $\xi_{0z,z}$ is the initial stretch factor of the fiber under the loading force Mg/N of the test mass. Advanced LIGO will use the fused silica fibers with the following parameters: $r = 2 \times 10^{-4} m$, $M = 40$ kg, $E = 72$ GPa, $l = 0.6$ m, and $N = 4$ fibers per test mass. These parameters produce the bending length $\lambda \simeq 0.001$ m $\ll l$.

The periodic solutions of the homogeneous Eq. (29) can be written as

$$\eta(z, t) \propto e^{i\omega t} e^{pz}, \quad (31)$$

where

$$p^2 = \frac{1 \pm \sqrt{1 + 4(\frac{\omega\lambda}{c_s})^2}}{2\lambda^2}. \quad (32)$$

For frequencies of interest, $\omega\lambda/c_s \ll 1$, and thus the solutions feature two physically distinct branches, $p = \pm 1/\lambda$ and $p = \pm i\omega/c_s$. The former branch represents evanescent quasistatic bending perturbations that will be large near the fiber's attachment points, while the latter represents tension waves in a fiber. The boundary conditions $\eta(0) = \eta'(0) = \eta'(l)$ and $\eta(l) = X_{\text{testmass}}$, together with $\lambda \ll l$, determine the full solution for the fiber:

$$\eta(z, t) = Be^{i\omega t}[\eta_{\text{bend}}(z) + \eta_{\text{wave}}(z)], \quad (33)$$

where

$$\eta_{\text{bend}}(z) = k\lambda\{e^{-\frac{z}{\lambda}} - [\cos(kl) + k\lambda \sin(kl)]e^{\frac{z-l}{\lambda}}\}, \quad (34)$$

and

$$\eta_{\text{wave}}(z) = \sin(kz) - k\lambda \cos(kz). \quad (35)$$

Here $k = \omega/c_s$, and the amplitude B is given by

$$B \simeq X_{\text{testmass}}(\omega)/\sin(kl) = X_{\text{testmass}}(\omega)/\sin(\pi\omega/\omega_s). \quad (36)$$

Therefore, in the Fourier domain the readout variable is given by

$$X_{\text{readout}}(\omega) = -\lim_{\epsilon\to 0+}\frac{1}{2\pi i(\omega - i\epsilon)}\frac{gVx_c}{N\pi r^2} \times \frac{1}{\pi\frac{\omega}{\omega_s}\cos[\pi\frac{\omega}{\omega_s}]\omega_p^2 - \omega^2\sin[\pi\frac{\omega}{\omega_s}]} \times [\lambda^{-2}\eta_{\text{bend}}(z,\omega) - k^2\eta_{\text{wave}}(z,\omega)], \quad (37)$$

where $\eta_{\text{bend}}(z,\omega)$ and $\eta_{\text{wave}}(z,\omega)$ are given by Eqs. (34) and (35), respectively. In the time domain, putting in all the damping terms, I get

$$X_{\text{readout}}(t) = C_p(x_c,z)[1-\cos(\omega_p t)e^{-\gamma_p t}] + \Sigma_{j=1}^{\infty}C_{vj}(x_c,z)[1-\cos(\omega_{vj}t)e^{-\gamma_{vj}t}], \quad (38)$$

where

$$C_p(x_c,z) = -\frac{gVx_c}{N\pi r^2\omega_p^2}\left(\frac{e^{-\frac{z}{\lambda}} - e^{\frac{z-l}{\lambda}}}{\lambda l} - \frac{\omega_p^2}{\omega_s^2}\frac{\pi^2}{l^2}\frac{z}{l}\right), \quad (39)$$

and

$$C_{vj}(x_c,z) = \frac{2gVx_c(-1)^{j+1}}{N\pi r^2\omega_{vj}^2}\times\left\{\frac{\pi j}{\lambda l}[e^{-\frac{z}{l}} - (-1)^j e^{\frac{z-l}{\lambda}}] - \left(\frac{\pi j}{l}\right)^2\sin(\pi jz/l)\right\}. \quad (40)$$

In the expressions above I used $\lambda \ll l$ and $\omega_p \ll \omega_s$. I remind the reader that x_c, z are the coordinates of the location of the creep event with the effective volume V, and that Eq. (38) gives the test-mass response to such an event. The geometric nature of the prefactors in Eqs. (39) and (40) is apparent once one recalls $g/\omega_p^2 \simeq l$, and $g/\omega_{vj}^2 \simeq [Nm/M](\pi j)^{-2}l$.

It is instructive to compute a numerical example. In the expression (38) above, consider values $x_c = r$, $V = \text{nm}^3$, and $z = 0$ (i.e., a formation of a nanometer-size hole at the top edge of the fiber). The displacement that one then gets at a pendulum frequency is of order 10^{-21} m.

It is worthwhile to have another look at the right-hand side of Eq. (37). The part of the equation in square brackets,

$$C(z,\omega) = \lambda^{-2}\eta_{\text{bend}}(z,\omega) - k^2\eta_{\text{wave}}(z,\omega) \quad (41)$$

determines the z dependence of the coupling of the creep event to the horizontal motion of the test mass. The function $C(z)$ is plotted in Fig. 1, for $\omega = \omega_s$ (i.e., the fundamental violin mode). Fiducial parameters that were used in making the plot are specified in the figure's header. The function peaks very strongly within λ from the attachment ends of the fiber; there $C(z) \sim k/\lambda$ is dominated by the η_{bend}.

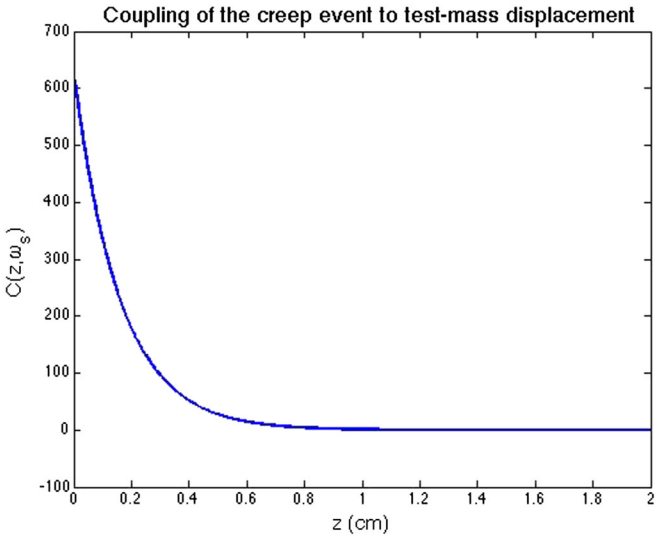

FIG. 1 (color online). The quantity $C(z,\omega)$, which characterizes the coupling strength of the creep event to the test-mass horizontal displacement, is plotted as a function of the creep event's distance from the top of the fiber, at a frequency of the fundamental violin mode. The coupling is strongly peaked within the bending length λ from the top. A similar "bending" peak occurs at the bottom of the suspension fiber (not shown). The parameters for the plot are those for advanced LIGO suspension fused silica fibers: $E = 72$ GPa, $r = 2\times10^{-4}$ m, $l = 0.6$ m, $M = 40$ kg, $N = 4$.

Away from the attachment points, the coupling is dominated by the η_{wave} part of the solution and $C(z) \sim k^2$.

In this subsection's model the creep events are assumed to be triggered homogeneously in the suspension fibers [34]. Thus the creep events have only $\sim\lambda/l$ chance to be triggered within λ from the attachment points. However, they have individually a much larger impact [by a factor of $1/(k\lambda)$] on the test-mass motion then those originating away from the attachments. It follows that the creep events originating within the bending regions near attachment points contribute most of the creep noise; their contribution is greater by a factor of $\sim k^{-2}l^{-1}\lambda^{-1} = (l/\pi^2\lambda)(\omega_s/\omega)$ than that of the creep events away from the attachment points. This is studied in Sec. IV.

C. The case of a nonorthogonal laser beam and suspension fiber

Let us now consider the case where a laser beam is inclined by a small angle β with respect to the horizontal direction. This is an inevitable effect because of the spherical shape of the equipotential surface on which the test masses in the same arm are located; for a 4 km arm $\beta \simeq 3\times10^{-4}$ radians. It is this misalignment that was previously thought to be the major source of the creep noise [16]; we treat this mechanism within the formalism developed in the previous section. The reciprocal force applied at the test mass now has a vertical component

$$F_{\rm vert}(t) = -\beta\Theta(t) \tag{42}$$

that causes the vertical test-mass motion

$$X_{\rm vert} = -\frac{\beta l\Theta(t)}{N\pi Er^2}[1-\cos(\omega_{\rm vert}t)e^{-\gamma_{\rm vert}t}], \tag{43}$$

where the negative sign corresponds to the upward motion. Here we take into account only one vertical suspension mode with the angular frequency

$$\omega_{\rm vert} = \sqrt{\frac{NE\pi r^2}{Ml}} \tag{44}$$

and the damping rate $\gamma_{\rm vert}$; the higher-order vertical modes are at a much higher frequency and have a much weaker coupling to the sudden force. The readout variable from Eq. (26) is given by

$$X_{\rm vertreadout}(t) = \frac{MgV\beta\Theta(t)}{E(N\pi r^2)^2}[\cos(\omega_{\rm vert}t)e^{-\gamma_{\rm vert}t}-1]. \tag{45}$$

In the Fourier domain,

$$X_{\rm vertreadout}(\omega) = \frac{\beta gV}{N\pi r^2 l}\frac{1}{2\pi i\omega[\omega_{\rm vert}^2-(\omega-i\gamma_{\rm vert})^2]}. \tag{46}$$

It is instructive to compare the amplitude of the vertical mode to the amplitude of the pendulum mode excited by the creep even near the attachment point, as inferred from Eq. (38). Their ratio is approximately given by

$$\frac{\text{vertical}}{\text{pendulum}} \simeq \frac{\beta r^2}{x_c\lambda} \sim \text{few}\times 10^{-5}. \tag{47}$$

It is the smallness of this ratio that makes the contribution to the creep noise from the creep-induced fiber lengthening subdominant relative to the direct horizontal coupling, in most of the LIGO band.

IV. CREEP NOISE IN THE STATIONARY LIMIT

Consider now a situation where multiple creep events are triggered in sequence. According to the central limit theorem, if the events occur sufficiently frequently, their superposition produces a random Gaussian noise in the test-mass motion. The response of the test mass to a single creep event can be written as $X(\vec{\alpha}, t-t_0)$ where t_0 is the time when the creep event is triggered, and $\vec{\alpha}$ is the set of parameters characterizing the event (location in the fiber, effective volume, etc.). In what follows we assume that the creep events are statistically independent from one another and that the creep-event parameters sample some well-defined probability distribution function. This assumption is known not to hold in some systems that exhibit so-called ''crackle noise'' [35], and will be relaxed in future work. If the probability density distribution $P(\vec{\alpha})$ is time invariant, then the creep noise is stationary and has a spectral density given by

$$S_X(f) = 8\pi^2 R\int d\vec{\alpha}|X(\vec{\alpha},\omega)|^2P(\vec{\alpha}), \tag{48}$$

where R is the rate of the creep events. The $d\vec{\alpha}$ implies a multidimensional integral over the parameter space of $\vec{\alpha}$. Evaluating this expression for the model of the cylindrical fiber, we get

$$S_x(f) = \frac{2R\langle V^2\rangle}{c_s^2}\left(\frac{g}{2\pi Nr}\right)^2\times Q(\omega-i\gamma)G(k), \tag{49}$$

where

$$Q(\omega) = \left|\pi\frac{\omega}{\omega_s}\cos\left(\pi\frac{\omega}{\omega_s}\right)\omega_p^2-\omega^2\sin\left(\pi\frac{\omega}{\omega_s}\right)\right|^{-2} \tag{50}$$

and

$$G(k) = \frac{1}{\lambda l}\{[1+\cos^2(kl)]+k\lambda[2\sin(2kl)+kl]\}. \tag{51}$$

Here $\langle V^2\rangle$ is the ensemble average of the (volume)^2 of the creep events in the system. Naturally, this quantity is meaningful only in our simple model for the creep events; however, a term like this, representing the mean of the squared intensity of the creep events, is expected in any generic model for the localized creep events. The first term in square brackets on the right-hand side of the above equations is due to creep events generated near the attachment points, while the second term is due to creep events generated in the fiber's bulk; in both of these the terms of order $k\lambda$ have been neglected. It is clear that the noise is strongly dominated by the creep events near the attachment point.

The spectral density of noise due to the vertical lengthening of the fibers is given by

$$S_{\rm xvert}(f) = \frac{2R\langle V^2\rangle\beta^2}{\omega^2}\left(\frac{g}{N\pi r^2 l}\right)^2 Q_{\rm vert}(\omega-i\gamma), \tag{52}$$

where

$$Q_{\rm vert}(\omega) = |\omega_{\rm vert}^2-\omega^2|^{-2}. \tag{53}$$

The plots for $\sqrt{S_x(f)}$ and $\sqrt{S_{\rm xvert}(f)}$ are shown in Fig. 2. While the scale on the vertical axis of these plots is arbitrary, since $R\langle V^2\rangle$ is unknown, the spectral density shape and the relative contribution of the two noises are fixed. We observe that the direct horizontal coupling induces greater creep noise than the vertical motion, at all frequencies except at a narrow band around $f = \omega_{\rm vert}/(2\pi)$.

V. DISCUSSION

In this paper I have provided an elastodynamic calculation of the interferometer's response to a creep event, and found the functional form of the creep noise in the stationary limit. A simple model where the fiber was modeled

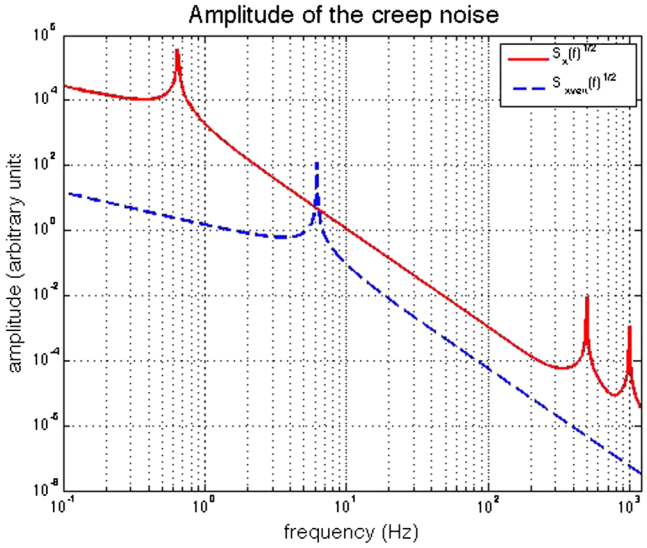

FIG. 2 (color online). Two amplitudes of the creep noise are plotted: that due to the direct horizontal coupling (continuous), and that due to the vertical lengthening of the suspension fibers (dashed). While the units on the y axis are arbitrary, the ratio of the two contributions depends on the elastodynamics only and is robust. One can see that the horizontal coupling makes a dominant contribution everywhere except in a narrow band near the vertical resonance of the last stage of the suspension. The parameters for the plot are those for advanced LIGO suspension fused silica fibers: $E = 72$ GPa, $r = 2 \times 10^{-4}$ m, $l = 0.6$ m, $M = 40$ kg, $N = 4$. For this plot, the Q factor of all the modes is taken to be 10^3; this choice affects the height of the sharp peaks in the figure. Realistic Q values will be several orders of magnitude higher.

as a cylinder of constant radius was considered in detail, since this allowed me to obtain analytical expressions for the test-mass response. Two interrelated qualitative features of this model are worth noting: (1) Creep events near the fiber's ends receive a much stronger test-mass response in the LIGO band than those at the center of the fiber, and contribute the majority of the creep noise; and (2) the dominant coupling to the interferometer's readout is via excitation of the violin and pendulum modes of the suspension, and not via the lengthening of the fiber. I should caution though that these conclusions may not hold in a fiber with a more complex dependence of the cross-sectional radius r on the height z. In particular, the fibers in advanced LIGO suspensions are made significantly thicker near the end points, in order to minimize the suspension's thermal noise. This thickening will reduce the local tension stress, thus reducing both the coupling of a creep event to the test-mass motion and the likelihood of a creep event.

In a simple model for the creep noise, I have assumed that the creep events are triggered homogeneously in the suspension fiber. This may not be the case. The creep events may be triggered preferentially (1) at the locations where the fiber is welded to the test mass or the upper suspension plate, although this is not very likely since at the weld the fiber is much thicker than at its center ($r = 1.5 \times 10^{-3}$ m), so the tension is small [25]; or (2) near the locations where the ears that support the test mass are bonded to it. The bonding material is nonmetallic and nonglassy and is a potential source of problems [24]. In future work I plan to explore the spatial distribution of the expected creep events, as well as relax the assumption of their statistical independence. I plan to also deal with the issues of non-Gaussianity of the creep-event triggers; it can presumably be mitigated by considering the output of several independent interferometers.

Some comfort for the advanced interferometers can be derived from the fact that experiments [19,22,23] have not observed any influence of the creep noise on the violin-mode motion. We note, however, that all of the measurements in question have searched for the creep noise at high frequencies corresponding to the resonant frequencies of violin modes, from several hundred to several thousand hertz. If the creep events are statistically independent from each other, then the expected creep noise is red, with $\sqrt{S_X(f)} \propto f^{-3}$ except near resonances; see Eqs. (49) and (50). This is the same scaling as that for the suspension thermal noise in the case where damping of the fiber's motion is structural (see, e.g., Ref. [36]). Therefore, one may argue that since no creep noise that exceeds the suspension thermal noise is observed at high frequencies, none is expected to exceed the suspension thermal noise at low frequencies as well. This argument, however, relies on a very simple model for the creep noise that was developed in Sec. IV, and in particular it relies on the creep events being statistically independent. This assumption does not hold in many systems that release their free energy via spontaneous acoustic emission events (known as the crackle noise); see Ref. [35] and references therein. Thus further experimental and theoretical work is warranted for the low-frequency domain.

ACKNOWLEDGMENTS

I thank Vladimir Braginsky for impressing on me the importance of nonstationary noise in many a conversation that we have had from the first time we met in September 1994. I thank Misha Gorodetsky for his insightful comments given as part of the internal LSC review for this article. I thank Riccardo DeSalvo, Eric Gustafson, Jan Harms, Norna Robertson, and Peter Saulson for comments on the earlier version of this manuscript. I thank Rana Adhikari, Yanbei Chen, Kip Thorne, and Sergei Vyatchanin for useful discussions. Finally, I thank Sarah Levin for proofreading parts of the manuscript before submission. The calculations in this paper were completed during a visit to the LIGO laboratory at Caltech. The research was supported by the Australian Research Council Future Fellowship.

APPENDIX: RESPONSE OF THE SUSPENSION TO A PERIODIC FORCE APPLIED AT THE TEST MASS

Here we provide a quick derivation; similar derivations for more complicated situations when the test-mass tilt is allowed are given in e.g., Appendix A of Ref. [37]. Suppose a periodic force

$$F = F_0 e^{i\omega t} \tag{A1}$$

is acting on the test mass and induces its periodic motion

$$X_{\text{testmass}} = X_0 e^{i\omega t}. \tag{A2}$$

The fiber's motion is given by

$$\eta(z, t) = \frac{\sin(kz)}{\sin(kl)} X_0 e^{i\omega t}. \tag{A3}$$

Here $k = \omega/c_s = (\pi/l)\omega/\omega_s$ is the tension-wave vector. The horizontal component of the backreaction tension force acting on the test mass is

$$F_{\text{fiber}} = F_{f0} e^{i\omega t} = -Mgk\cot(kl) X_0 e^{i\omega t}. \tag{A4}$$

The second Newton's law gives

$$F_0 + F_{f0} = -M\omega^2 X_0. \tag{A5}$$

Substituting Eq. (A4) above we get

$$X_0 = \frac{F_0}{M} \frac{1}{gk\cot(kl) - \omega^2}, \tag{A6}$$

which is equivalent to Eq. (20) in the text.

[1] B. P. Abbott *et al.*, Rep. Prog. Phys. **72**, 076901 (2009).
[2] F. Acernese *et al.*, Classical Quantum Gravity **25**, 114045 (2008).
[3] H. Luck, *Proceedings of the Twelfth Marcel Grossman Meeting on General Relativity*, edited by T. Damour, R. T. Jantzen, and R. Ruffini (World Scientific, Singapore, 2010).
[4] K. Arai *et al.* (TAMA Collaboration), J. Phys. Conf. Ser. **120**, 032010 (2008).
[5] G. Harry *et al.*, Classical Quantum Gravity **27**, 084006 (2010).
[6] T. Accadia, in *Proceedings of the Rencontres de Moriond Conference, 2011* (unpublished).
[7] J. Abadie *et al.*, Classical Quantum Gravity **27**, 173001 (2010).
[8] M. W. Coughlin and J. Harms, arXiv:1202.4826.
[9] *Optical Coatings and Thermal Noise in Precision Measurements*, edited by G. Harry, T. Bodiya, and R. DeSalvo (Cambridge University Press, Cambridge, England, 2012).
[10] H. J. Kimble, Y. Levin, A. B. Matsko, K. S. Thorne, and S. P. Vyatchanin, Phys. Rev. D **65**, 022002 (2001).
[11] A. Buonanno and Y. Chen, Phys. Rev. D **64**, 042006 (2001).
[12] Gravitational-wave interferometers represent a relatively new field and one has to be vigilant for the possibility that an important noise source has been overlooked. As a historical example, thermal noise was thought to be well understood in the 1990s. However, Harry *et al.* [13] (following an earlier suggestion of Ref. [14]) demonstrated the importance of the coating thermal noise, while Braginsky, Gorodetsky, and Vyatchanin [15] discovered the importance of thermoelastic noise in sapphire test masses. These discoveries then both revolutionized thermal-noise research and changed the projected noise budgets for the interferometers.
[13] G. M. Harry *et al.*, Classical Quantum Gravity **19**, 897 (2002).
[14] Y. Levin, Phys. Rev. D **57**, 659 (1998).
[15] V. B. Braginsky, M. Gorodetsky, and S. P. Vyatchanin, Phys. Lett. A **264**, 1 (1999).
[16] G. Cagnoli, L. Gammaitoni, J. Kovalik, F. Marchesoni, M. Punturo, S. Braccini, R. De Salvo, F. Fidecaro, and G. Losurdo, Phys. Lett. A **237**, 21 (1997).
[17] A. Yu. Ageev, I. A. Bilenko, V. B. Braginsky, and S. P. Vyatchanin, Phys. Lett. A **227**, 159 (1997).
[18] I. A. Bilenko, A. Yu. Ageev, and V. B. Braginsky, Phys. Lett. A **246**, 479 (1998).
[19] A. Gretarsson and P. R. Saulson, Rev. Sci. Instrum. **76**, 054502 (2005).
[20] R. DeSalvo, *Second Edoardo Amaldi Conference Gravitational Waves*, edited by G. Coccia, G. Veneziano, and G. Pizzella (World Scientific, Singapore, 1997), p. 228.
[21] S. Aston *et al.*, Classical Quantum Gravity **29**, 235004 (2012).
[22] I. A. Bilenko and S. L. Lourie, Phys. Lett. A **305**, 31 (2002).
[23] B. Sorazu, K. A. Strain, I. S. Heng, and R. Kumar, Classical Quantum Gravity **27**, 155017 (2010).
[24] R. DeSalvo (private communication).
[25] N. Robertson (private communication).
[26] J. D. Achenbach, *Reciprocity in Elastodynamics* (Cambridge University Press, Cambridge, England, 2003).
[27] Y. Levin and M. van Hoven, Mon. Not. R. Astron. Soc. **418**, 659 (2011).
[28] Naturally, other time dependencies may also be considered within this formalism.
[29] More precisely, for frequencies such that the corresponding sound waves have a much larger wavelength than the size of V, which is an excellent approximation in our situation.
[30] Strictly speaking, this expression is valid only to zeroth order in m/M at low frequencies, where m and M are the

masses of the string and the test mass, respectively. This is of order of 10^{-4} for LIGO.

[31] This enforces causality of the test-mass response. In case there is no damping, one needs to use the Landau rule when evaluating the inverse Fourier transform: the integration contour should pass under every pole.

[32] R. D. Blandford and K. S. Thorne, Applications of Classical Physics, online course at http://www.pma.caltech.edu/Courses/ph136/yr2011 (2011).

[33] L. D. Landau and E. M. Lifshitz, *Theory of Elasticity* (Pergamon, Oxford, 1986), 3rd ed.

[34] In real suspension systems, this may not be so.

[35] K. A. Dahmen, Y. Ben-Zion, and J. T. Uhl, Phys. Rev. Lett. **102**, 5501D (2009).

[36] G. I. Gonzalez and P. R. Saulson, J. Acoust. Soc. Am. **96**, 207 (1994).

[37] V. B. Braginsky, Y. Levin, and S. P. Vyatchanin, Meas. Sci. Technol. **10**, 598 (1999).